

# INTEGRATION OF LASER AND PHOTOGRAMMETRIC DATA FOR CALIBRATION PURPOSES

A. F. Habib<sup>a</sup>, M. S. Ghanma<sup>a</sup>, M. F. Morgan<sup>a</sup>, E. Mitishita<sup>b</sup>

<sup>a</sup> Department of Geomatics Engineering, University of Calgary  
2500, University Drive NW, Calgary AB T2N 1N4 Canada – (habib, mghanma)@geomatrics.ucalgary.ca, mfmorgan@ucalgary.ca,

<sup>b</sup> Departamento de Geomática, Universidade Federal Do Paraná, Caixa Postal 19.001, 81.531-970 Curitiba, Paraná, Brasil  
mitishita@ufpr.br

## TS – PS: WG I/5 Platform and Sensor Integration

**KEY WORDS:** Laser scanning, Registration, Calibration, Fusion, Feature, Modelling

### ABSTRACT:

Laser scanners are becoming popular since they provide fast and dense geometric surface information. However, sudden elevation changes along the surface are not clearly visible in the laser data due to the sparse distribution of captured points. In general, laser data provides high density surface information in homogenous areas and low density surface information elsewhere (i.e., object space break-lines). Photogrammetry, on the other hand, provides less dense surface information but with high quality, especially along object space discontinuities. Hence, a natural synergy of both systems can be inferred and consequently integration of the respective data would lead to higher quality surface information than that obtained through the use of a single sensor. However, prior to such integration, both systems should be precisely calibrated and aligned. The calibration is usually carried-out for each system independently using additional control information. In this paper, the calibration of the laser and photogrammetric systems is evaluated by checking the quality of fit between co-registered photogrammetric and laser surfaces. The paper starts by introducing a registration procedure where a set of linear features is extracted from both sets. First, planar surfaces from laser data are extracted and adjacent planes are intersected to determine three-dimensional straight line segments. Secondly, linear features from the photogrammetric dataset are obtained through aerial triangulation. A mathematical model for expressing the necessary constraints for the alignment of conjugate photogrammetric and laser straight lines is established. The model ensures that corresponding straight lines will be collinear after registering the two datasets relative to a common reference frame. The quality of fit between the registered surfaces is then used to evaluate and/or improve the calibration parameters of the photogrammetric and laser systems. In this paper, an experiment with real data is used to illustrate this concept. The registered surfaces in this example revealed the presence of systematic inconsistencies between the photogrammetric and laser systems. The pattern of these inconsistencies is found to resemble the effect of un-calibrated lens distortion. In this case, the laser data is used as control information for the determination of lens distortion, which when considered leads to a better fit between the registered surfaces. The estimated lens distortion using the laser was found to be very close to that determined through a rigorous camera calibration procedure.

## 1. INTRODUCTION

Laser scanners are becoming an increasingly accepted tool for acquiring 3D point clouds that represent scanned objects with millimetre precision. As can be inferred from the name, laser scanning is a non-contact range measurement based on emitting a laser light pulse and instantaneously detecting the reflected signal. This should be coupled with high-quality GPS/INS units for tracking the position and orientation of the range finder as it scans over objects and surfaces under consideration.

The sparse and positional nature of laser data makes it ideal for mapping homogeneous surfaces but lacks the ability to capture objects' break-lines with reliable quality. Another drawback is that laser data has no inherent redundancy and its planimetric accuracy is worse than the vertical (Maas, H.-G., 2002), in addition to little or no semantic information. However, the continuous development of laser systems, in the aspect of reduced hardware size and increased resolution and density, makes it an increasingly favoured option in a variety of applications especially where rapid and accurate data collection on physical surface is required (Schenk and Csathó, 2002).

On the other side, photogrammetric data is characterized by high redundancy through observing the desired features in multiple images making it more suited for mapping heavily

populated areas. Richness in semantic information and dense positional information along object space break lines add to its advantages. Nonetheless, photogrammetry has its own drawbacks; where there is almost no positional information along homogeneous surfaces and vertical accuracy is worse than the planimetric accuracy. A major existing obstacle in the way of automation in photogrammetry is the complicated and sometimes unreliable matching procedures, especially when dealing with large scale imagery over urban areas.

It can be clearly observed that both, photogrammetry and laser data, have unique characteristics that make them preferable in certain applications. One can notice that a disadvantage in one technology is contrasted by an opposite strength in the other. Hence, integrating the two systems would lead to higher quality surface information (Baltasvias, 1999). However, the complementary information can be fully utilized only after precise calibration of both systems, which is separately implemented for each system. The synergy would be considered complete after aligning the photogrammetric and laser data models relative to a common reference frame. (Habib and Schenk, 1999; Postolov et al., 1999).

This paper introduces a registration procedure through which the calibration of photogrammetric and laser scanning systems is assessed. The suggested technique emphasizes the type and

extraction of registration primitives in addition to the registration steps required to reveal any calibration discrepancies in the systems.

Most registration methodologies use discrete points as the sole primitive for solving the registration problem between two datasets. Such methodologies are not applicable to laser scanned surfaces since they correspond to laser footprints instead of distinct points that could be identified in imagery (Baltasvias, 1999). Conventionally, surface-to-surface registration and comparison have been achieved by interpolating both datasets into a uniform grid. The comparison is then reduced to estimating the necessary shifts by analyzing the elevations at corresponding grid posts (Ebner and Ohlhof, 1994; Kilian et al., 1996). Several issues can arise with this approach. First, the interpolation to a grid will introduce errors, especially when dealing with captured surfaces over urban areas. Moreover, minimizing the differences between the surfaces along the z-direction is only valid when dealing with horizontal planar surfaces (Habib and Schenk, 1999). Postolov et al. (1999) presented another approach, which works on the original scattered data without prior interpolation. However, the implementation procedure involves an interpolation of one surface at the location of conjugate points on the other surface. Additionally, the registration is based on minimizing the differences between the two surfaces along the z-direction. Schenk (1999) introduced an alternative approach, where distances between points of one surface along surface normals to locally interpolated patches of the other surface are minimized. Habib and Schenk (1999) and Habib et al. (2001) implemented this methodology within a comprehensive automatic registration procedure. Such an approach is based on processing the photogrammetric data to produce object space planar patches. This might not be always possible since photogrammetric surfaces provide accurate information along object space discontinuities while supplying almost no information along homogeneous surfaces with uniform texture.

In this paper, the registration procedure will utilize straight line primitives and 3D similarity transformation for aligning the photogrammetric model relative to the laser data reference frame. The following section previews the components of the general registration paradigm and the particulars of applying each component to the photogrammetric and laser datasets under consideration. The last two sections cover the experimental results as well as the conclusions and recommendations for future work.

## 2. METHODOLOGY

The registration process aims at combining multiple datasets acquired by different sensors in order to reach better accuracy and enhanced inference about the environment than could be attained through using only one sensor. The following subsections address the components and issues necessary for an effective registration paradigm (Brown, 1992).

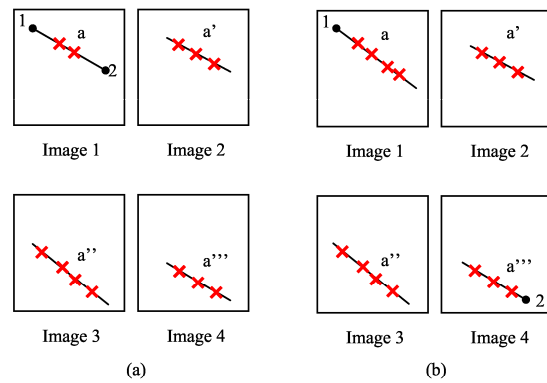
### 2.1 Registration primitives

To register any two datasets, certain common features have to be identified and extracted from both sets. Such features will subsequently be used as the registration primitives relating the datasets together. The type of chosen primitives greatly influences subsequent registration steps. Hence, it is crucial to first decide upon the primitives to be used for establishing the transformation between the datasets in question. In this paper,

straight line features are selected for this purpose. This choice is motivated by the fact that such primitives can be reliably, accurately, and automatically extracted from photogrammetric and laser datasets. The procedure adopted to extract straight lines from the photogrammetric and laser datasets and how they are included in the overall alignment procedure is described below.

**Photogrammetric straight line features:** The representation scheme of 3D straight lines in the object and image space is central to the methodology for producing such features from photogrammetric datasets. Representing object space straight lines using two points along the line is the most convenient representation from a photogrammetric point of view since it yields well-defined line segments (Habib et al., 2002). On the other hand, image space lines will be represented by a sequence of 2-D coordinates of intermediate points along the feature. This appealing representation can handle image space linear features in the presence of distortions as they will cause deviations from straightness. Furthermore, it will allow for the inclusion of linear features in scenes captured by line cameras since perturbations in the flight trajectory would lead to deviations from straightness in image space linear features corresponding to object space straight lines (Habib et al., 2002).

Manipulating tie straight lines appearing in a group of overlapping images begins by identifying two points in one (Figure 1a) or two images (Figure 1b) along the line under consideration. These points are then used to define the corresponding object space line segment. It is worth mentioning that these points need not be identifiable or even visible in other images. Intermediate points along the line are measured in all overlapping images. Similar to the end points, the intermediate points need not be conjugate, Figure 1.



- End points defining the line in object space
- × Intermediate points

Figure 1. End points defining the object line are either measured in one image (a) or two images (b).

The relationship between the image coordinates of the line end points  $\{(x_1, y_1), (x_2, y_2)\}$  and the corresponding ground coordinates  $\{(X_1, Y_1, Z_1), (X_2, Y_2, Z_2)\}$  is established through the collinearity equations. Hence, four equations are written for each line. The intermediate points are included into the adjustment procedure through a mathematical constraint, which states that the vector from the perspective centre to any intermediate image point along the line is contained within the plane defined by the perspective centre of that image and the two points defining the straight line in the object space, Figure 2. That is to say, for a given intermediate point, a

constraint that indicates the points  $\{(X_1, Y_1, Z_1), (X_2, Y_2, Z_2), (X_{O_1}, Y_{O_1}, Z_{O_1})\}$  and  $(x_i, y_i, 0)$  are coplanar, is introduced and mathematically described by Equation 1.

$$(\vec{V}_1 \times \vec{V}_2) \cdot \vec{V}_3 = 0 \quad (1)$$

In the above equation,  $\vec{V}_1$  is the vector connecting the perspective centre to the first end point along the object space line,  $\vec{V}_2$  is the vector connecting the perspective centre to the second end point along the object space line, and  $\vec{V}_3$  is the vector connecting the perspective centre to an intermediate point along the corresponding image line. It is important to note that the three vectors should be represented relative to a common coordinate system (e.g., the ground coordinate system). The constraint in Equation 1 incorporates the image coordinates of the intermediate point, the Exterior Orientation Parameters (EOP), the Interior Orientation Parameters (IOP) including distortion parameters, as well as the ground coordinates of the points defining the object space line. Such a constraint does not introduce any new parameters and can be written for all intermediate points along the line in the imagery. The number of constraints is equal to the number of intermediate points measured along the image line.

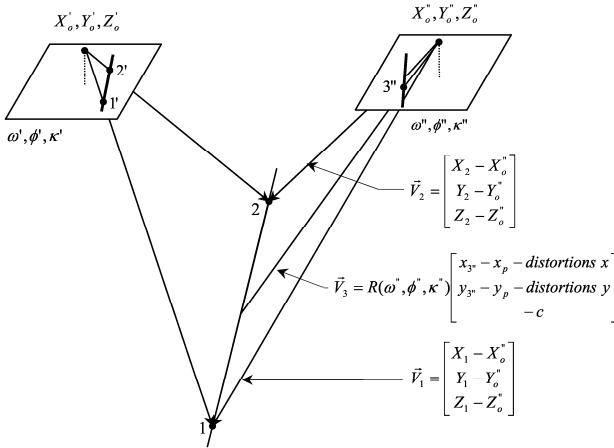


Figure 2. Perspective transformation between image and object space straight lines and the coplanarity constraint for intermediate points along the line.

In some applications, photogrammetric lines are used as control lines instead of being regular tie lines. In this situation, the object coordinates of line end points are known, hence, these points need not be measured in any of the images. Consequently, image space linear features are represented only by a group of intermediate points measured in all images.

After the identification and extraction of straight lines from imagery, a photogrammetric model is generated through a photogrammetric triangulation using an arbitrary datum without any control information. This arbitrary datum is defined by fixing seven coordinates of any three well-distributed points.

**Laser straight line features:** The increasing recognition of laser scanning as a favourable data acquisition tool by the photogrammetric community led to a number of studies aiming at pre-processing laser data. The major goal of such studies ranges from simple primitive detection and extraction to more complicated tasks such as segmentation, and perceptual organization (Csathó et al., 1999; Lee and Schenk, 2001; Filin, 2002).

In this paper, laser straight line features will be used as a source of control to align the photogrammetric model. To extract such lines, suspected planar patches in the laser dataset are manually identified with the help of corresponding optical imagery, Figure 3. The selected patches are then checked using a least-squares adjustment to determine whether they are planar or not, and to remove blunders. Finally, neighbouring planar patches with different orientation are intersected to determine the end points along object space discontinuities between the patches under consideration.

The datum for the laser lines is directly established by a combination of high-quality GPS/INS units installed onboard of the sensor platform.

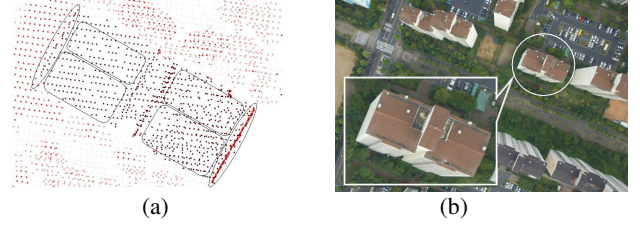


Figure 3. Manually identified planar patches in the laser data (a) guided by the corresponding optical image (b).

## 2.2 Registration transformation function

At this point, a photogrammetric model is generated from the photogrammetric triangulation using an arbitrary datum without knowledge of any control information. In addition, a set of conjugate photogrammetric-laser lines has been manually identified. These lines, in both datasets, are identified by their end points. It is important to reiterate that the end points of such conjugate lines are not required to be conjugate.

An essential property of any registration technique is the type of transformation or mapping function adopted to properly overlay the two datasets. In this paper, a 3D similarity transformation is used as the registration transformation function, Equation 2. Such transformation assumes the absence of systematic biases in both photogrammetric and LIDAR surfaces (Filin, 2002). However, the quality of fit between conjugate primitives can be analyzed to investigate the presence of such behaviour.

$$\begin{bmatrix} X_A \\ Y_A \\ Z_A \end{bmatrix} = \begin{bmatrix} X_T \\ Y_T \\ Z_T \end{bmatrix} + S R(\Omega, \Phi, K) \begin{bmatrix} X_a \\ Y_a \\ Z_a \end{bmatrix} \quad (2)$$

where:

$S$  is the scale factor,  $(X_T Y_T Z_T)^T$  is the translation vector between the origins of the photogrammetric and laser data coordinate systems,  $R(\Omega, \Phi, K)$  is the 3D orthogonal rotation matrix between the two coordinate systems,  $(X_a Y_a Z_a)^T$  are the photogrammetric point coordinates, and  $(X_A Y_A Z_A)^T$  are the coordinates of the corresponding point relative to the laser data reference frame.

## 2.3 Similarity measure

The role of the similarity measure is to mathematically express the relationship between the attributes of conjugate primitives in overlapping surfaces. The similarity measure formulation depends on the selected registration primitives and their respective attributes as well as the transformation function. In

this paper, the similarity measure formulation has been incorporated in mathematical constraints ensuring the coincidence of conjugate linear features after establishing the proper co-registration between involved surfaces.

Referring to Figure 4, the two points describing the line segment from the photogrammetric model undergo a 3D similarity transformation onto the line segment from the laser dataset. The objective here is to introduce the necessary constraints to describe the fact that the model segment (12) coincides with the object segment (AB) after applying the absolute orientation transformation function.

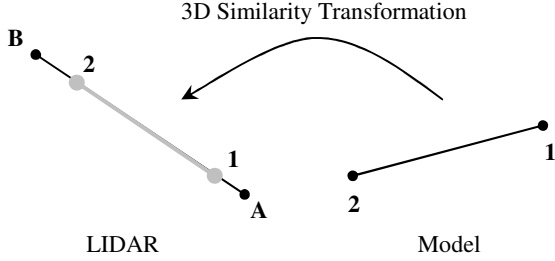


Figure 4. Similarity measure between photogrammetric and laser linear features.

For the photogrammetric point (1), this constraint can be mathematically described as in Equation 3.

$$\begin{bmatrix} X_T \\ Y_T \\ Z_T \end{bmatrix} + S R_{(\Omega, \Phi, K)} \begin{bmatrix} X_1 \\ Y_1 \\ Z_1 \end{bmatrix} = \begin{bmatrix} X_A \\ Y_A \\ Z_A \end{bmatrix} + \lambda_1 \begin{bmatrix} X_B - X_A \\ Y_B - Y_A \\ Z_B - Z_A \end{bmatrix} \quad (3)$$

Equation 4 shows the constraint for point (2).

$$\begin{bmatrix} X_T \\ Y_T \\ Z_T \end{bmatrix} + S R_{(\Omega, \Phi, K)} \begin{bmatrix} X_2 \\ Y_2 \\ Z_2 \end{bmatrix} = \begin{bmatrix} X_A \\ Y_A \\ Z_A \end{bmatrix} + \lambda_2 \begin{bmatrix} X_B - X_A \\ Y_B - Y_A \\ Z_B - Z_A \end{bmatrix} \quad (4)$$

where  $\lambda_1$ , and  $\lambda_2$  are scale factors.

Subtracting Equation 4 from Equation 3 yields:

$$(\lambda_2 - \lambda_1) \begin{bmatrix} X_B - X_A \\ Y_B - Y_A \\ Z_B - Z_A \end{bmatrix} = S R_{(\Omega, \Phi, K)} \begin{bmatrix} X_2 - X_1 \\ Y_2 - Y_1 \\ Z_2 - Z_1 \end{bmatrix} \quad (5)$$

Dividing both parts of Equation 5 by  $(\lambda_2 - \lambda_1)$  and substituting  $\lambda$  for  $S/(\lambda_2 - \lambda_1)$ , Equation 6 is produced. Equation 6 emphasizes the concept that model line segments should be parallel to the object line segments after applying the rotation matrix. To recover the elements of the rotation matrix, Equation 6 is further manipulated and rearranged by dividing the first and second rows by the third to eliminate  $\lambda$ , Equations 7.

$$\begin{bmatrix} X_B - X_A \\ Y_B - Y_A \\ Z_B - Z_A \end{bmatrix} = \lambda R_{(\Omega, \Phi, K)} \begin{bmatrix} X_2 - X_1 \\ Y_2 - Y_1 \\ Z_2 - Z_1 \end{bmatrix} \quad (6)$$

$$\begin{aligned} \frac{(X_B - X_A)}{(Z_B - Z_A)} &= \frac{R_{11}(X_2 - X_1) + R_{12}(Y_2 - Y_1) + R_{13}(Z_2 - Z_1)}{R_{31}(X_2 - X_1) + R_{32}(Y_2 - Y_1) + R_{33}(Z_2 - Z_1)} \\ \frac{(Y_B - Y_A)}{(Z_B - Z_A)} &= \frac{R_{21}(X_2 - X_1) + R_{22}(Y_2 - Y_1) + R_{23}(Z_2 - Z_1)}{R_{31}(X_2 - X_1) + R_{32}(Y_2 - Y_1) + R_{33}(Z_2 - Z_1)} \end{aligned} \quad (7)$$

A pair of conjugate line segments yields two equations, which contribute towards the estimation of two rotation angles, the azimuth and pitch, along the line. On the other hand, the roll angle across the line cannot be estimated due to singularities. Hence a minimum of two non-parallel lines is needed to recover the three elements of the rotation matrix ( $\Omega, \Phi, K$ ), Figure 5.

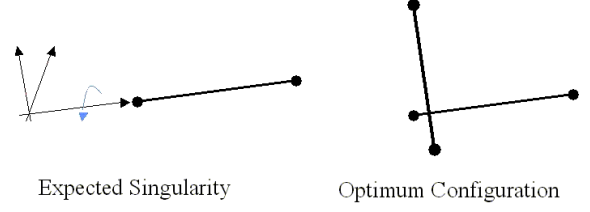


Figure 5. Singular and optimum configuration to recover rotation angles

To determine the scale factor and the shift components, apply the rotation matrix to the coordinates of the first point defining the photogrammetric line, which yields Equation 8.

$$\begin{bmatrix} X_T \\ Y_T \\ Z_T \end{bmatrix} + S \begin{bmatrix} x_1 \\ y_1 \\ z_1 \end{bmatrix} = \begin{bmatrix} X_A \\ Y_A \\ Z_A \end{bmatrix} + \lambda_1 \begin{bmatrix} X_B - X_A \\ Y_B - Y_A \\ Z_B - Z_A \end{bmatrix} \quad (8)$$

where,

$$\begin{bmatrix} x_1 \\ y_1 \\ z_1 \end{bmatrix}^T = R_{(\Omega, \Phi, K)} \begin{bmatrix} X_1 \\ Y_1 \\ Z_1 \end{bmatrix}^T$$

Rearranging the terms yields:

$$\lambda_1 \begin{bmatrix} X_B - X_A \\ Y_B - Y_A \\ Z_B - Z_A \end{bmatrix} = \begin{bmatrix} X_T + S x_1 - X_A \\ Y_T + S y_1 - Y_A \\ Z_T + S z_1 - Z_A \end{bmatrix} \quad (9)$$

In Equation 9, eliminate  $\lambda_1$  by dividing the first and second rows by the third, Equations 10. The same applies to point 2 and Equations 11 can be written.

$$\frac{(X_B - X_A)}{(Z_B - Z_A)} = \frac{(X_T + S x_1 - X_A)}{(Z_T + S z_1 - Z_A)}, \quad \frac{(Y_B - Y_A)}{(Z_B - Z_A)} = \frac{(Y_T + S y_1 - Y_A)}{(Z_T + S z_1 - Z_A)} \quad (10)$$

$$\frac{(X_B - X_A)}{(Z_B - Z_A)} = \frac{(X_T + S x_2 - X_A)}{(Z_T + S z_2 - Z_A)}, \quad \frac{(Y_B - Y_A)}{(Z_B - Z_A)} = \frac{(Y_T + S y_2 - Y_A)}{(Z_T + S z_2 - Z_A)} \quad (11)$$

Combining Equations 10 and 11 produces the two independent constraints as shown in Equations 12.

$$\begin{aligned} \frac{(X_T + S x_1 - X_A)}{(Z_T + S z_1 - Z_A)} &= \frac{(X_T + S x_2 - X_A)}{(Z_T + S z_2 - Z_A)} \\ \frac{(Y_T + S y_1 - Y_A)}{(Z_T + S z_1 - Z_A)} &= \frac{(Y_T + S y_2 - Y_A)}{(Z_T + S z_2 - Z_A)} \end{aligned} \quad (12)$$

Equations 12 can be written for each line in one dataset and its conjugate in the other. Consequently, two pairs of line segments yielding four equations are required to solve for the four unknowns. If the lines were intersecting, the shift components can be estimated (using the intersection points) but the scale factor cannot be recovered. As a result, at least two non-coplanar line segments are needed to recover these parameters, Figure 6.

In summary, a minimum of two non-coplanar line segments is needed to recover the seven elements of the 3D similarity transformation.

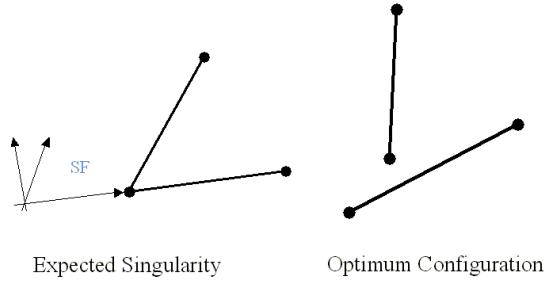


Figure 6. Singular and optimum configuration to recover scale and shift components

At this point, the components of the registration paradigm have been addressed. Straight line segments are chosen as the registration primitives along with a 3D similarity transformation function. Also, the similarity measure is formulated based on the selected primitives and transformation function. The quality of fit, represented by the resulting variance component from the similarity measure as well as the residuals and discrepancy between conjugate features, will be used to validate and check the quality of the calibration parameters associated with the imaging and ranging systems.

### 3. EXPERIMENTAL RESULTS

In order to verify the methodology and procedure, imagery and laser data over an urban area were collected, Figure 7.



Figure 7. Aerial image of area under consideration

CANON EOS 1D digital camera (pixel size =  $11.5\mu\text{m}$ , focal length =  $28.469051\text{ mm}$ ) was used to capture twenty-three overlapping images in three flight lines. Based on a flying height of  $200\text{ m}$ , a base of  $70\text{ m}$ , and assuming a one pixel measurement error, the expected planimetric accuracy is estimated as  $0.09\text{ m}$  while the vertical accuracy is expected to be  $0.36\text{ m}$  with an overall spatial accuracy of  $0.37\text{ m}$ . From the laser scanner hardware and mission specifications, the spatial laser data accuracy is expected to be in the range of  $0.35\text{ m}$ . With the above anticipated accuracies, the surfaces are expected to have a discrepancy in the range of  $0.5\text{ m}$ .

Straight line segments as well as some tie points were measured as described earlier and then incorporated in a bundle adjustment procedure with an arbitrary datum. The output of the bundle adjustment included the ground coordinates of tie points in addition to the ground coordinates of points defining the object space line segments.

In the laser data, homogeneous patches have been manually identified to correspond to that of selected features in imagery.

Planar surfaces are then fitted through the selected patches, from which neighbouring planar surfaces are intersected to produce object space line segments. A total of twenty-three well distributed 3D edges within the area of interest have been identified along ten buildings from three laser strips.

Least-squares adjustment is then used to solve for the parameters of the 3D similarity transformation function and the results are shown in Table 1. A visual presentation of datasets after transformation is shown in Figure 8.

Scale	1.008609	$\pm 0.002245$
$X_T$ (m)	4.81	$\pm 0.74$
$Y_T$ (m)	-1.24	$\pm 0.45$
$Z_T$ (m)	-30.05	$\pm 0.44$
$\Omega$ ( $^\circ$ )	1.892336	$\pm 0.132785$
$\Phi$ ( $^\circ$ )	1.315345	$\pm 0.354789$
$K$ ( $^\circ$ )	0.320431	$\pm 0.094157$

Table 1. 3D similarity parameters between laser and photogrammetry models.

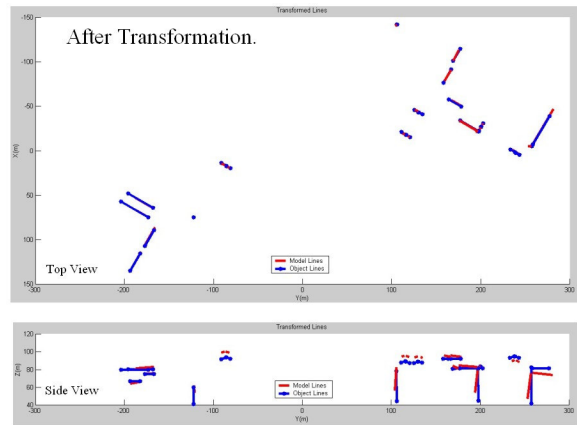


Figure 8. Aerial photogrammetric and laser datasets after transformation

To assess the quality of fit, the mean normal distance between the laser and transformed photogrammetric line segments turned out to be  $3.27\text{ m}$ , a surprisingly poor result considering the camera, flight mission, and laser scanner specifications. The expected surface fit was in the range of a sub-meter.

A closer look at the side view in Figure 8, the discrepancy revealed that the pattern of deviation between the laser and photogrammetric features is similar to deformations arising from ignored radial lens distortion. To determine the radial lens distortion of the implemented camera, two alternatives were followed. The first alternative implemented the laser features as control information within the bundle adjustment procedure in a self-calibration mode allowing for the derivation of an estimate for the radial lens distortion. The estimated radial lens distortion coefficient turned out to be  $-6.828 \times 10^{-5} \text{ mm}^{-2}$ . The second alternative determined an estimate of the radial lens distortion through a bundle adjustment with self-calibration involving imagery captured from a test field with numerous control points, which had been surveyed earlier. The estimated radial lens distortion coefficient turned out to be  $-6.913 \times 10^{-5} \text{ mm}^{-2}$ , which is almost identical to the value determined by implementing the laser features as control within the photogrammetric bundle adjustment. Afterwards, the registration procedure had been

repeated after considering the radial lens distortion. The new parameters of the transformation function are presented in Table 2.

After considering the radial lens distortion, the mean normal distance between the laser and transformed photogrammetric line segments turned out to be 0.58 m, which is within the expected accuracy range. A sharp drop in the standard deviations of the transformation function parameters also took place as can be seen when comparing Tables 1 and 2. The overall improvement in the spatial discrepancies after introducing the radial lens distortion verifies its existence.

Scale	1.018032	$\pm 0.000663$
$X_T$ (m)	7.05	$\pm 0.18$
$Y_T$ (m)	2.42	$\pm 0.13$
$Z_T$ (m)	-24.27	$\pm 0.11$
$\Omega$ (°)	4.926549	$\pm 0.034478$
$\Phi$ (°)	0.603525	$\pm 0.092137$
$K$ (°)	0.214818	$\pm 0.029516$

Table 2. 3D similarity parameters between laser and photogrammetry models after distortion compensation.

#### 4. CONCLUSIONS AND RECOMMENDATIONS

Analyzing the previous results, a set of conclusions can be extracted from this study, mainly; the efficiency of the suggested registration procedure in identifying the systematic discrepancies between the involved surfaces. After a closer look at the discrepancies' behaviour, it was possible to justify the cause and take the necessary remedial measures to remove such errors. Also, straight line features proved its suitability to establish a common reference frame for the laser and photogrammetric surfaces, a result that has been suggested by prior research work. The involved datasets in the experimental section illustrated the compatibility between laser and photogrammetric surfaces. However, it is important to precisely calibrate both systems to guarantee the absence of systematic biases. In addition, the two surfaces must be relative to the same reference frame as a prerequisite for any further integration between the two datasets. For example optical imagery can be rendered onto the laser data to provide a realistic 3D textured model of the area of interest.

Further research is required to address the automatic extraction of different types of primitives from the surfaces in question. Developing an automatic matching strategy between laser-derived and photogrammetric features is an interesting extension. For example, Modified Iterated Hough Transform (MIHT) can be used to simultaneously determine the correspondence between conjugate primitives in overlapping surfaces and the parameters involved in the registration transformation function. The type of transformation function will also be looked at. So far, 3D similarity transformation has been assumed as the registration transformation function relating overlapping surfaces. Future work will investigate the discrepancy pattern for different errors and factors such as GPS/INS/Laser spatial and rotational biases or biases in the IOP of the involved cameras.

#### 5. REFERENCES

- Baltsavias, E., 1999. A comparison between photogrammetry and laser scanning, *ISPRS Journal of Photogrammetry & Remote Sensing*, 54(1):83-94.
- Brown, L. G., 1992. A survey of image registration techniques, *ACM computing surveys*, 24(4):325-376.
- Csathó, B. M., K. Boyer, and S. Filin, 1999. Segmentation of laser surfaces, *International Archives of Photogrammetry and Remote Sensing*, 32(3W14):73-80.
- Ebner, H., and T. Ohlhof, 1994. Utilization of ground control points for image orientation without point identification in image space, *International Archives of Photogrammetry and Remote Sensing*, 30(3/1):206-211.
- Filin, S., 2002. Surface clustering from airborne laser scanning data, *International Archives of Photogrammetry and Remote Sensing*, 32(3A):119-124.
- Habib, A., and T. Schenk, 1999. New approach for matching surfaces from laser scanners and optical sensors, *International Archives of Photogrammetry and Remote Sensing*, 32(3W14):55-61.
- Habib, A., Y. Lee, and M. Morgan, 2001. Surface matching and change detection using the modified Hough transform for robust parameter estimation, *Photogrammetric Record Journal*, 17(98): 303-315.
- Habib, A., Y. Lee, and M. Morgan, 2002. Bundle adjustment with self-calibration using straight lines, *Photogrammetric Record Journal*, 17(100): 635-650.
- Kilian, J., N. Haala, and M. Englich, 1996. Capture and evaluation of airborne laser scanner data, *International Archives of Photogrammetry and Remote Sensing*, 31(B3):383-388.
- Lee, I., and T. Schenk, 2001. 3D perceptual organization of laser altimetry data, *International Archives of Photogrammetry and Remote Sensing*, 34(3W4):57-65.
- Maas, H.-G., 2002. Methods for measuring height and planimetry discrepancies in airborne laserscanner data, *Photogrammetric Engineering and Remote Sensing*, 68(9):933-940.
- Postolov, Y., A. Krupnik, and K. McIntosh, 1999. Registration of airborne laser data to surfaces generated by photogrammetric means, *International Archives of Photogrammetry and Remote Sensing*, 32(3W14):95-99.
- Schenk, T., 1999. Determining transformation parameters between surfaces without identical points, *Technical Report Photogrammetry No. 15*, Department of Civil and Environmental Engineering and Geodetic Science, OSU, 22 pages.
- Schenk, T., and B. Csathó, 2002. Fusion of LIDAR data and aerial imagery for a more complete surface description, *International Archives of Photogrammetry and Remote Sensing*, 34(3A):310-317.

#### 6. ACKNOWLEDGEMENTS

The authors would like to thank Mosaic Mapping Inc, for supplying the aerial and laser datasets on which the experimental work was conducted.